Cloning and identification of MYPT3: a prenylatable myosin targetting subunit of protein phosphatase 1

Jeffrey A. SKINNER and Alan R. SALTIEL[1]

Department of Cell Biology, Pfizer Global Research and Development, Ann Arbor Laboratories, 2800 Plymouth Road, Ann Arbor, MI 48105, U.S.A., and Department of Physiology, Life Sciences Institute, University of Michigan School of Medicine, 1150 West Medical Center Drive, Ann Arbor, MI 48109-0650, U.S.A.

To identify novel protein phosphatase 1 (PP1)-interacting proteins, a yeast two-hybrid 3T3-L1 adipocyte cDNA library was screened with the catalytic subunit of PP1 as bait. In the present work, the isolation, identification and initial biochemical characterization of a novel PP1-interacting protein, MYPT3, which is homologous with the myosin phosphatase targetting subunit (MYPT) family, is described. MYPT3 aligns $> 99\%$ with a region of mouse genomic DNA clone RP23-156P23 and localizes to chromosome 15, between markers at 44.1–46.5 cM, as demonstrated by radiation hybrid mapping. The gene consists of ten exons that encode for a 524-amino acid sequence with a predicted molecular mass of 57529 Da. The N-terminal region of MYPT3 consists of a consensus PP1-binding site and multiple ankyrin repeats. MYPT3 is distinguished from related $\sim$ 110–130 kDa MYPT subunits by its molecular mass of 58 kDa, and a unique C-terminal region that contains several potential signalling motifs and a CaaX prenylation site. We have shown that affinity-purified glutathione S-transferase (GST)–MYPT3 is prenylated by purified recombinant farnesyltransferase *in vitro*. Endogenous PP1 from 3T3-L1 lysates specifically interacts with MYPT3. Additionally, purified PP1 activity was inhibited by GST–MYPT3 toward phosphorylase *a*, myosin light chain and myosin substrate *in vitro*. Overall, our findings identify a novel prenylatable subunit of PP1 that defines a new subfamily of MYPT.

Key words: 3T3-L1 adipocytes, ankyrin repeats, farnesylation, protein phosphatase 1, yeast two-hybrid.

INTRODUCTION

Protein phosphatase 1 (PP1) is a serine/threonine phosphatase that plays a key role in various cellular functions, including cell cycle progression, muscle contraction, gene expression, glycogen metabolism and neurotransmission [1–3]. In mammalian cells, the catalytic subunit of PP1 is regulated by distinct regulatory protein subunits that directly inhibit activity or target the enzyme to a specific subcellular localization or substrate [3,4]. The 'inhibitory' family of regulatory subunits consists of inhibitor-1 [5,6], its homologue DARPP-32 [7], inhibitor-2 [5,6] and NIPP-1 [8,9]. In addition, the catalytic subunit of PP1 associates independently with 'targetting' subunits that regulate its localization to subcellular compartments or its substrate specificity. Major targetting subunits include the glycogen-binding subunits G_M [10,11], G_L [12,13] and protein targetting to glycogen (PTG) [14], the phosphatase 1 nuclear targetting subunit ('PNUTS') [15], and the myosin phosphatase targetting subunits MYPT1 and MYPT2 [16–20]. Overall, more than 20 targetting subunits of PP1 have been identified in mammalian tissue and *Saccharomyces cerevisiae* by various methods, such as standard protein purification, screening yeast two-hybrid cDNA libraries, or affinity-purification with immobilized microcystin or the catalytic subunit of PP1.

PP1 is found in many cellular compartments, including the nucleus, plasma membrane, glycogen particles and myofibrils. Compartmentalization of PP1 is only understood mechanistically for several known targetting subunits, which do not fully account for the diverse intracellular actions of PP1. This suggests that additional targetting subunits may exist. To identify novel PP1-interacting proteins, we screened a 3T3-L1 adipocyte cDNA library with PP1 as bait, utilizing the yeast two-hybrid method. We describe, in the present work, the cloning and identification of a novel prenylatable protein, which contains a variant PP1-binding consensus sequence and is approx. 30–40 % identical to the N-terminal region of the myosin phosphatase targetting (MYPT) subunit family. Designated MYPT3, this DNA sequence encodes for a 524-amino-acid protein with a predicted molecular mass of 57529 Da. Although homologous, MYPT3 is distinguished from MYPT1/2 by biochemical properties that suggest a unique role in the regulation of myosin light-chain (MLC) phosphorylation.

EXPERIMENTAL

Materials

Purified recombinant farnesyltransferase and purified haemagglutinin (HA)-tagged H-Ras (wild type) were generously provided by Dr Patrick Casey (Duke University Medical Center, Durham, NC, U.S.A). Dr Timothy Haystead (Duke University, Durham, NC, U.S.A) kindly provided a construct for a 110 kDa glutathione S-transferase (GST)–M110 isoform truncated at the C-terminus [18], affinity purified MLC kinase from rabbit skeletal muscle [21] and purified recombinant calmodulin [22]. Bacterial lysate containing recombinant PP1-α, and glutathione–agarose-purified GST–PTG were gifts from Dr Matthew Brady (Pfizer, Ann Arbor, MI, U.S.A.) [14,23]. Purified ($> 95\%$) recombinant human PP1-γ was purchased from Calbiochem. Affinity-purified chicken anti-PP1 antibody was

Abbreviations used: DOBA, drop out base with agar; FPP, farnesylpyrophosphate; HA, haemagglutinin; GST, glutathione S-transferase; MLC, myosin light chain; MYPT, myosin phosphatase targetting subunit; PP1, protein phosphatase 1; PTG, protein targetting to glycogen.

[1] To whom correspondence should be addressed at Department of Physiology, Life Sciences Institute, University of Michigan School of Medicine, 1150 West Medical Center Drive, Ann Arbor, MI 48109-0650, U.S.A. (e-mail saltiel@umich.edu).

The nucleotide sequence for MYPT3 will appear in DDBJ, EMBL and GenBank® databases under the accession number AY010723.

a gift from Dr J. Lawrence, Jr. (University of Virginia, Charlottesville, VA, U.S.A.). Microcystin-LR and farnesylpyrophosphate (FPP) were purchased from Biomol Research Laboratories (Plymouth Meeting, PA, U.S.A.), [^{3}H]FPP was obtained from NEN Life Science Products (Boston, MA, U.S.A.). Enhanced chemiluminescence reagents, the expression vector pGEX-4T-3, and glutathione–Sepharose 4B beads were purchased from Pharmacia. Mouse anti-GST monoclonal antibodies were purchased from Santa Cruz Biotechnology. Goat anti-rabbit IgG-horseradish peroxidase and rabbit anti-mouse IgG-horseradish peroxidase secondary antibodies were purchased from Bio-Rad Laboratories. All other materials were purchased from Sigma unless stated.

Buffers

Lysate buffers consisted of 1 mM sodium orthovanadate, 10 mM sodium pyrophosphate, 10 mM sodium fluoride, and the following protease inhibitors: 1 mM benzamidine, 0.1 mM PMSF, 1 μg/ml Pepstatin A, 20 μg/ml trypsin inhibitor, 100 μg/ml Pefabloc-SC (Boehringer-Mannheim), and 0.5 μg/ml leupeptin.

Yeast two-hybrid screening

The entire open-reading frame of the PP1 catalytic subunit (α-isoform) was previously subcloned into the bait vector pGBT9 (Clontech) containing a GAL4 DNA-binding domain [14]. A 3T3-L1 adipocyte cDNA library was synthesized with a cDNA synthesis kit (Stratagene), and ligated unidirectionally into the *Eco*RI-*Xho*I multiple cloning sites of pGAD-GH GAL4 activation domain vector (Clontech) [14]. Y190 yeast were sequentially transformed with pGBT9-PP1 followed by the pGAD-GH-3T3-L1 cDNA library, as described previously [14,24]. Briefly, a single-Y190 colony containing pGBT9-PP1 was incubated overnight with 300 ml of yeast extract peptone dextrose media at 30 °C. These cells were made competent in 100 mM lithium acetate and transformed with 120 μg of 3T3-L cDNA library in 25 % poly(ethylene glycol) for 30 min at 30 °C. Heat shock was performed for 30 min at 42 °C with added DMSO (6 % final concentration). Transformed cells were grown on DOBA (drop-out base with agar) plates (BIO 101) containing 30 mM 3-aminotriazole, but lacking leucine, tryptophan and histidine. Colonies appearing between days 4–5 of incubation at 30 °C were tested for β-galactosidase activity on DOBA plates containing 50 mM 3-aminotriazole and 80 mg/l 5-bromo-4-chloro-3-indolylphosphate-β-D-galactopyranoside (Gibco-BRL). Isolated DNA from β-galactosidase-active colonies was transformed into *Escherichia coli* HB101. Bacteria were grown on M9 minimal media agar plates lacking leucine. Isolated bacterial plasmids were transformed back into Y190 yeast cells for confirmation of β-galactosidase activity. Bacterial plasmids also were digested with *Eco*RI-*Xho*I and inserts were sequenced by the University of Michigan DNA Sequencing Core Facility. Complete sequencing of pGAD-clone 7X was performed with primers to the pGAD-5′ GAL4 AD region, pGAD-3′ region, and many -5′ and -3′ internal regions within the insert. At least three independent DNA sequences in each direction were obtained for sequencing. The nucleotide and deduced amino acid sequences were aligned with GenBank® databases using BLAST [25,26], and assembled into contigs using Sequencher 4.0 software (Gene Codes Corp., Ann Arbor, MI, U.S.A.). Identification of signalling motifs was performed using SMART [27,28], PROSITE [29] and Pfam 4.3 [30].

Radiation hybrid analysis

Whole genome radiation hybrid mapping of a mouse/hamster panel [31] was performed by PCR with a forward primer 5′-GACTGAGAGCTGCTGCATGAAGG-3′ and a reverse primer 5′-CAAGTGTCTGAGCTCTCACCAGAG-3′ (Research Genetics). Primers were synthesized to intron 1 and 3 regions of MYPT3, and specifically generated an approx. 400-bp PCR product from genomic mouse DNA. Data were compared with the Whitehead Institute/Massachusetts Institute of Technology Center for Genome Research's radiation hybrid map of the mouse genome for placement. Additional analysis was performed using the Mouse Genome Database [32].

Northern-blot analysis

Total cellular RNA was isolated from 3T3-L1 fibroblasts and differentiated adipocytes (day 4) by a single-step phenol-guanidine isothiocyanate method using TRIzol reagent (Gibco-BRL) [33]. Purified RNA (20 μg) was subjected to gel electrophoresis in 1.2 % agarose/2.2 M formaldehyde, then transferred overnight to Hybond membrane (Amersham Pharmacia) according to the NorthernMax™ protocol (Ambion). Primers were obtained by restriction digestion of pGAD-GH-clone 7X, followed by agarose-gel fractionation of either the 0.5 kb *Eco*RI-*Xho*I fragment or the complete 1.5 kb *Eco*RI-*Eco*RI fragment. Probes were labelled with [α-^{32}P]dCTP ($> 1 \times 10^9$ c.p.m./μg) using the random prime labelling system *redi*prime™ II (Amersham Pharmacia). Hybridizations were performed for 2 h at 55 °C with NorthernMax™ buffer (Ambion), washed extensively, and analysed by autoradiography. Alternatively, a mouse multiple-tissue Northern blot (MTN™; Clontech) was performed, with the indicated primers, according to the manufacturer's protocol.

Preparation of mouse tissue samples

Fresh tissue was obtained from FVB-N1 mice, homogenized by mincing in 25 mM Tris/HCl (pH 7.5), 1 mM EDTA, 50 mM NaF, 50 mM β-glycerophosphate, 1 mM sodium orthovanadate, and protease inhibitors. The lysate was diluted with loading buffer [50 mM Tris/HCl (pH 6.8), 10 % (v/v) glycerol, 1 mM EDTA, 3 % SDS and 0.5 mg/ml Bromophenol Blue], boiled and stored at −20 °C.

Generation of polyclonal MYPT3 peptide antibodies

To generate anti-MYPT3 antibodies, the peptide [C]QGRQRSLLRRRTSSAGSRGK (residues 328–347) was synthesized to include an N-terminal cysteine for site-directed keyhole-limpet haemocyanin conjugation and affinity purification. Antiserum was independently obtained from two immunized rabbits (Zymed Laboratories). Following a secondary immunization, antiserum was affinity purified with peptide-conjugated SulfoLink agarose, according to the manufacturer's instructions (Pierce). Purified anti-MYPT3 antibody was dialysed against 50 mM Tris/HCl (pH 7.5) in 50 % (v/v) glycerol, then stored at −20 °C.

Expression and purification of GST–MYPT3

The full-length open-reading frame of MYPT3 was excised from the isolated pGAD-GH-clone 7X plasmid using *Eco*RI and *Xho*I restriction enzymes, and subcloned into the pGEX-4T-3 expression vector (Pharmacia) using the same multiple cloning sites. Isolated plasmid was verified for proper in-frame cloning by DNA sequencing. The plasmid was transformed into BL21

cells (Gibco-BRL), then propagated by fermentation [550 rev./min; 2.5 lines/min ('lpm')] at 25 °C for approx. 16 h in 2 litres of Superbroth media (pH 7.2) supplemented with phosphates and 100 μg/ml ampicillin (Digene). Expression was induced with 0.1 mM isopropyl β-D-thiogalactoside (Gibco-BRL) for 5 h at 18 °C. Cells were centrifuged at 5000 ***g*** for 15 min, resuspended in 50 mM Hepes (pH 7.5), 5 mM EGTA/EDTA and protease inhibitors, then lysed by two passages through a French press. Cellular extracts were centrifuged for 30 min at 15000 ***g*** and the supernatant was incubated with glutathione–Sepharose 4B (Amersham Pharmacia). Beads were washed three times with 50 mM Hepes (pH 7.5), 5 mM EDTA/EGTA and then with 50 mM Tris/HCl (pH 7.4), 1 mM dithiothreitol. Protein was eluted with 30 mM glutathione in 50 mM Tris/HCl (pH 8.0), then dialysed against 50 mM Tris/HCl (pH 7.5), 50 % glycerol, 1 mM dithiothreitol and protease inhibitors. Following dialysis, the sample was centrifuged at 100000 ***g*** for 60 min at 4 °C, and the final soluble protein was stored at −20 °C. Protein concentrations of GST–MYPT3 was determined by the Bradford assay [34], and protein bands on polyacrylamide gels were revealed using Coomassie Blue stain.

Expression and purification of other GST fusion proteins

A GST–PTG fusion protein was expressed and purified as reported previously [14,23]. A recombinant 72.5 kDa fragment of the rat kidney M110 subunit of smooth muscle PP1M was expressed as a GST fusion protein and affinity purified on glutathione–agarose, as described previously [18]. The eluted protein was subjected to dialysis and ultracentrifugation, and was stored in a similar manner to GST–MYPT3.

In vitro farnesylation assay

Purified recombinant HA-Ras (0.5 μg), GST–MYPT3 (10 μg), or GST–M110-ΔC (15 μg) was incubated with purified recombinant farnesyltransferase (1 μg) for 30 min at 37 °C as described previously [35,36]. Each reaction mixture also contained 0.5 μM [^{3}H]FPP (10 Ci/mmol), 50 mM Tris/HCl (pH 7.5), 20 mM KCl, 5 mM $MgCl_2$, 5 μM $ZnCl_2$ and 2 mM dithiothreitol. Reactions were stopped by the addition of 4 % (w/v) SDS, precipitated with trichloroacetic acid and the mixture was passed through glass-fibre filters, as described previously [35,36]. Incorporation of [^{3}H]FPP was quantified by liquid scintillation spectroscopy of the dried filters. Amounts of [^{3}H]FPP incorporated were < 25 % of the total present per reaction mixture.

FLAG-tagged MYPT3 construct

The full-length open-reading frame of MYPT3 was sequentially excised from the yeast pGAD-GH-clone 7X plasmid with *Eco*RI and *Kpn*I, then subcloned into a pCMV-FLAG Tag 2A mammalian expression vector (Stratagene), using the same cloning sites. Isolated plasmid was verified for proper in-frame cloning by DNA sequencing.

Cell culture

3T3-L1 fibroblasts were maintained and differentiated into adipocytes as described previously [37]. Adipocytes were transiently transfected by electroporation, as described previously [38]. Plasmids used for electroporation was isolated from DH5α *E. coli* by caesium chloride double banding. Briefly, adipocytes were harvested by mild treatment with trypsin and electroporated with 500 μg of plasmid DNA under low-voltage conditions (160 V, 950 μF). Electroporated cells were allowed to recover for approx. 48 h before the experiments. A typical transfection efficiency of approx. 40–50 % was determined by electroporation of a *myc-LacZ* construct and β-galactosidase staining of cells.

Immunoprecipitation and immunoblotting

To prepare cellular extracts, 3T3-L1 adipocytes were washed twice with ice-cold PBS, then scraped from culture plates with homogenization buffer [50 mM Hepes (pH 7.4), 150 mM NaCl, 1 mM EDTA/EGTA, 10 % (v/v) glycerol, 1 % (v/v) Triton X-100] containing protease inhibitors, and centrifuged at 14000 ***g*** for 20 min at 4 °C. The supernatant was filtered through a 0.2 μm Millex-GV syringe filter (Millipore), then assayed for protein content. Equal protein (1.5 mg) from cellular lysates were pre-cleared with Protein A/G Plus Agarose (Santa Cruz Biotechnology) for at least 1 h, then incubated with 5 μg of primary antibody with fresh Protein A/G beads, overnight at 4 °C. After washing three times with homogenization buffer, the immune complex was solubilized with Laemmli sample buffer. Soluble protein was separated by SDS/PAGE and transferred on to a nitrocellulose membrane overnight at 25 V. Immunoblots were probed with specified primary antibodies and revealed by enhanced chemiluminescence following incubation with secondary antibodies linked to horseradish peroxidase. Before reprobing, membranes were soaked for 30 min at 55 °C with 60 mM Tris/HCl (pH 7.0), 2 % (w/v) SDS and 0.7 % (v/v) 2-mercaptoethanol.

GST fusion protein binding experiments

Approximately equal amounts of a bacterial lysate containing recombinant PP1 or 3T3-L1 lysates were pre-cleared with glutathione–Sepharose beads for 2 h at 4 °C. The supernatant was mixed with 25 μg GST–MYPT3, GST–PTG or fresh glutathione–Sepharose beads alone for 1 h at 4 °C. The complex was washed three times in lysis buffer, solubilized in Laemmli buffer, then fractionated by SDS/PAGE and transferred on to nitrocellulose membrane overnight at 25 V.

Phosphatase assays

Phosphatase assays with 1 nM PP1 (γ-isoform) were conducted at 30 °C with 5 μM ^{32}P-labelled phosphorylase *a* in assay buffer [50 mM Tris/HCl (pH 7.5), 1 mM $MnCl_2$, 0.3 % 2-mercaptoethanol, 1 % glycerol, 1 mg/ml BSA]. Alternatively, phosphatase assays with 7.5 nM PP1 were conducted for 15 min at 30 °C with 20 μM ^{32}P-labelled MLC or 1 μM ^{32}P-labelled myosin in assay buffer with 100 mM KCl added. Serial dilutions of GST–MYPT3 were pre-incubated with PP1γ for 10 min at 30 °C, and the reactions were initiated by adding pre-equilibrated substrate. Assays were terminated by adding 200 μl of ice-cold 20 % (w/v) trichloroacetic acid. Following the addition of 50 μl of 10 mg/ml BSA, the samples were centrifuged at 12000 ***g*** for 5 min, and the acid-soluble ^{32}[P]P_i was quantified by liquid scintillation counting.

Preparation of ^{32}P-labelled substrates

[^{32}P]Phosphorylase *a* (approx. 2000 c.p.m./pmol) was prepared as described previously [37]. Chicken gizzard myosin (Sigma) was phosphorylated as described previously [18]. As with myosin, purified bovine muscle MLC (Sigma) was labelled with 15 μg/μl MLC kinase for 1 h at 30 °C in reactions containing 50 mM Tris/HCl (pH 7.5), 1 mM EDTA, 1 mM $CaCl_2$, 25 mM $MgCl_2$,

1 mM dithiothreitol, 1 mM [γ-^{32}P]ATP (approx. 3500 c.p.m./pmol) and 5 μM calmodulin. Labelled myosin and MLC was dialysed extensively against phosphatase assay buffer and stored at 4 °C. The average stoichiometry of phosphorylation (expressed as mol phosphate/mol protein) was approx. 0.9 for phosphorylase *a* and 0.4 for myosin and MLC.

RESULTS

Identification of a PP1-interacting protein with the yeast two-hybrid system

To identify novel proteins interacting with the catalytic subunit of PP1, we screened a 3T3-L1 adipocyte cDNA library using the yeast two-hybrid system. The catalytic subunit of PP1 was cloned into the bait vector pGBT9, which contained a GAL4 DNA-binding domain, and sequentially transformed into the yeast Y190 strain with a 3T3-L1 adipocyte cDNA library fused to the GAL4 transcription activation domain 'prey' vector [14]. Of approx. 1.2×10^6 transformants, 31 of 107 selected colonies had β-galactosidase activity when plated on DOBA medium containing 5-bromo-4-chloro-3-indolylphosphate-β-D-galactopyranoside. DNA sequences from 15 positive colonies were assembled into a unique approx. 2.1 kb contig. Analysis of the contig sequence revealed a single open-reading frame defined by an initiation codon residing within a Kozak sequence [39,40] (5′-ACA TTC ACC ACC ATG GCC GAG-3′) and an in-frame stop codon, followed by approx. 272 bp of untranslated 3′-region, including a poly-A tail. The open-reading frame encodes for a 524-amino-acid sequence with a predicted molecular mass of 57529 Da (Figure 1). The entire open-reading frame was found intact in an isolated clone, referred to as clone 7X, which was used exclusively for characterization.

To determine the identity of the clone, we aligned the deduced amino-acid sequence of clone 7X with the non-redundant GenBank® peptide database. These alignments revealed a high degree of identity, approx. 30–40 %, with the N-terminal region of several MYPTs. The MYPT family is comprised of several

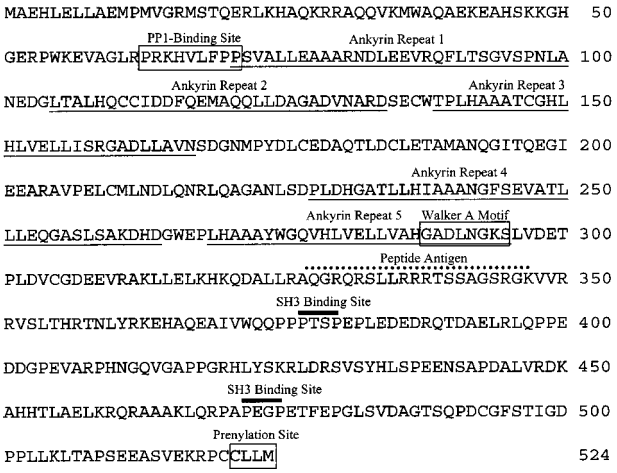

Figure 1 Structural analysis of the PP1-interacting protein

The deduced 524-amino acid sequence of clone 7X with a predicted molecular mass of 57529 Da. Structural analysis indicates several potential signalling motifs, as indicated, including a PP1 binding site (boxed), ankyrin repeats 1–5 (underlined), an ATP/GTP-binding (Walker A) site (boxed), two SH3-class I ligand binding consensus sites (thick line above the sequences), and a prenylation CaaX site (boxed). A peptide synthesized for antibody generation is indicated by a dotted line above the sequence.

approx. 110–130 kDa isoforms derived from alternative splicing of two independent genes, which are classified as MYPT1 or MYPT2 [41,42]. MYPTs contain a consensus PP1-binding site, consisting of four residues [K/R]-[V/I]-X-F [43], multiple ankyrin repeats that predominate the N-terminal region, and putative regulatory phosphorylation sites at Thr-654/Thr-695 (chicken gizzard MYPT2) [44]. An alignment of the protein product of clone 7X with representative members of the MYPT1/2 subfamilies is shown in Figure 2(A). Since both the PP1 binding site and multiple ankyrin repeats were similar to MYPT1/2, these data suggest its homology with MYPT (Figure 2A).

The 58 kDa gene product of clone 7X is approximately one-half the molecular mass of the known 110–130 kDa MYPT subunits. Without the C-terminal extension, the clone 7X gene product lacks the putative regulatory phosphorylation sites and leucine-zipper motif of MYPT2. In contrast, the C-terminal region of clone 7X contains several distinct signalling motifs not found in MYPT1/2 (Figure 2B). These include an ATP/GTP binding motif (Walker A type) and two independent SH3-binding consensus sites (class I ligands), which may suggest the potential for its regulation by nucleotides or interacting proteins. Another apparent distinction is a CaaX prenylation motif at the C-terminus of the clone 7X product. The CaaX motif is absent in known MYPT1/2 isoforms, and in other reported PP1 subunits. Thus the presence of a CaaX motif in the clone 7X product suggests its potential prenylation, which may represent a novel mechanism of PP1 targetting and regulation.

Designation of clone 7X as MYPT3

Sequence analysis of the clone 7X product further revealed its homology with several unidentified proteins, recently deduced from genomic sequencing. These homologous gene products include the human KIAA0823 protein (GenBank® accession number AB020630), the *Drosophila melanogaster* CG6896 gene product (GenBank® accession number AE003519), and the *Caenorhabditis elegans* K02A11 hypothetical protein (GenBank® accession number Z75544). Each of these deduced gene products contains multiple ankyrin repeats at its potential N-terminal region that are homologous with clone 7X. In addition, both the *Drosophila* and *C. elegans* gene products contain a similar PP1 binding site that is proximal to the N-terminus. Each also possesses a similar potential ATP/GTP binding site to the clone 7X product. The human KIAA0823 polypeptide lacks a PP1-binding site and an N-terminal methionine residue, which suggests the data represents an incomplete sequence. Interestingly, the C-terminus of each gene product contains a potential -CC or -CaaX prenylation motif, which is homologous with clone 7X. The C-terminal alignment of the deduced genomic products with clone 7X is shown in Figure 2(C). These observations suggest that a distinct and previously unidentified subfamily of myosin targetting subunits of PP1 exist in a variety of species.

BLAST searches of the GenBank® HTGS (high throughput genomic sequences) and EST (expressed sequence tag) nucleotide database show significant alignment of the clone 7X sequence with mouse genomic DNA. Clone 7X is > 99 % identical with 11 pieces of the mouse clone RP23-156P23 (GenBank® accession number AC074152), which is a recently updated working draft sequence. This observation suggests that we have identified a region of mouse genomic sequence (clone RP23-156P23, nt 95673–99449) as the gene encoding the clone 7X product. This region was previously unidentified and its chromosomal location unknown. The clone 7X coding region has 10 exons spanning

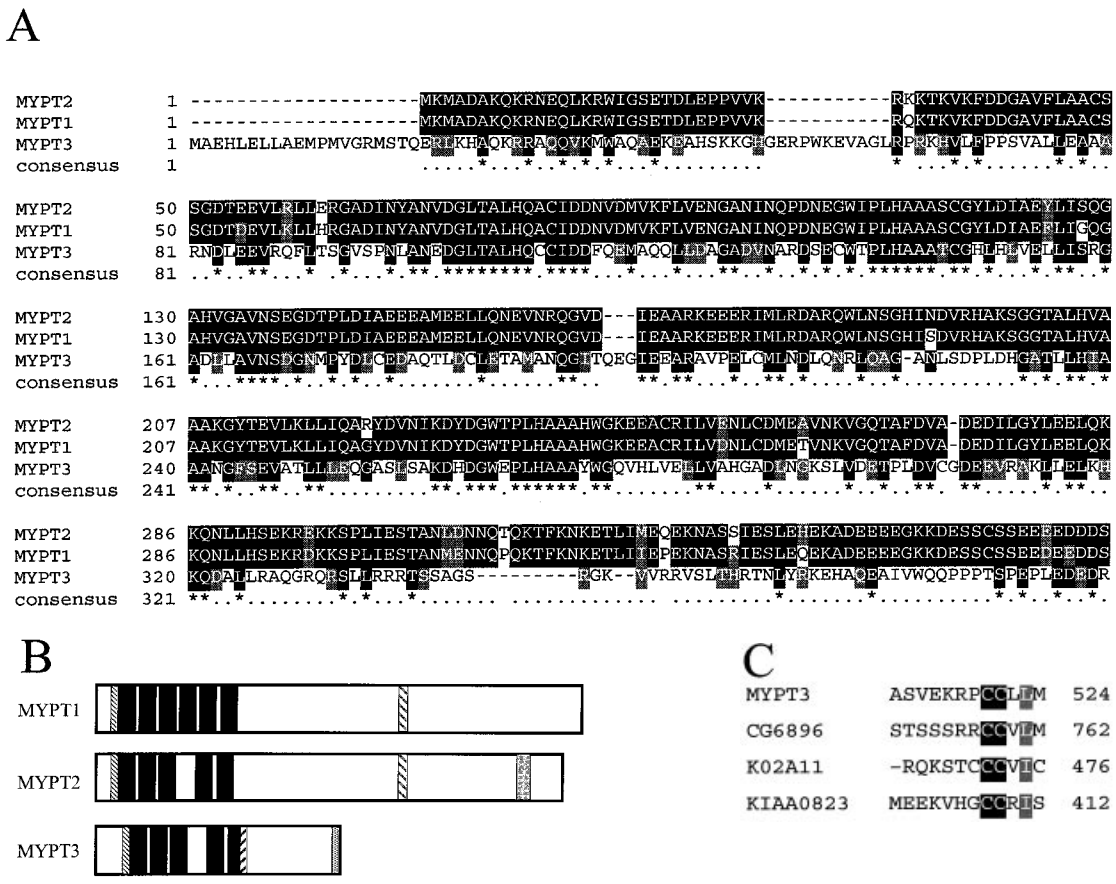

Figure 2 Identification of MYPT3

(**A**) The deduced protein sequence of Clone 7X is structurally homologous with the MYPT family. Shown are the N-terminal regions of the Clone 7X gene product (designated as MYPT3), the rat aorta MYPT 1 (GenBank® accession number S74907), and the chicken gizzard MYPT2 (GenBank® accession number D37986). (**B**) Schematic representation of the MYPT family. The boxed areas indicate the PP1 binding consensus site (▧), ankyrin repeat motifs (■), a putative ATP/GTP-binding (Walker A) site (▨), the regulatory Thr-654/Thr-695 phosphorylation sites (▧), a leucine zipper motif (▩), and the prenylation CaaX box (▨). (**C**) Alignment of the C-terminal CaaX motif of MYPT3, the deduced gene product CG6896 from *D. melanogaster* (GenBank® accession number AE003519), the *C. elegans* K02A11 hypothetical protein (GenBank® accession number Z75544), and the predicted human gene product KIAA0823 (GenBank® accession number AB020630).

3776 kb of mouse genomic sequence (Figure 3A). We also observed significant alignment ($\sim 85\%$) of mouse clone 7X with the human genomic clone RP11-349C2 (nt 95673–99449), which is a working draft sequence recently reported in the HTGS database. In this case, clone 7X aligns with 11 pieces of the human clone, representing approx. 4.7 kb of genomic coding sequence. Interestingly, the DNA sequence of KIAA0823 does not exactly align with RP11-349C2 (nt 95673–99449), suggesting multiple human homologues of clone 7X are likely. Overall, these observations suggest that clone 7X represents a unique mouse gene that encodes a previously unidentified protein with homology to the MYPT family. Thus we will refer to the clone 7X gene product as MYPT3.

Chromosomal mapping of MYPT3

To determine the chromosomal location of mouse MYPT3, a whole genome radiation hybrid panel of mouse/hamster cells [31] was mapped using synthetic primers based on regions of intron 1 and 3. Data obtained from this PCR analysis was compared with the Whitehead/Massachusetts Institute of Technology Center for Genome Research's radiation hybrid map of the mouse genome. Here we find placement of MYPT3 to chromosome 15, approx. 11.32 centiray (cR) (270 kb per cR_3000) from the marker D15Mit188 [logarithm of odds (lod) > 3.0)]. Analysis of the Mouse Genome Database [32] places the coding region between markers 44.1–46.5 centimorgans (cM), near several known genes such as Dia1 at 45.2 cM. A condensed mouse genetic map with placement of MYPT3 is shown in Figure 3(B). This region of mouse chromosome 15 is known to have homology with either human chromosome 8 or 22, as reported in the Mouse Genome Database [32]; however, more detailed data is necessary for further analysis.

Distribution of MYPT3

To assess the tissue distribution of MYPT3 mRNA, we hybridized a Northern blot of multiple mouse tissues with a 0.5 kb *Eco*RI-*Eco*RI fragment generated from clone 7X. A single MYPT3 mRNA transcript of approx. 3.2 kb was recognized predominately in heart, brain, lung, liver, skeletal muscle and

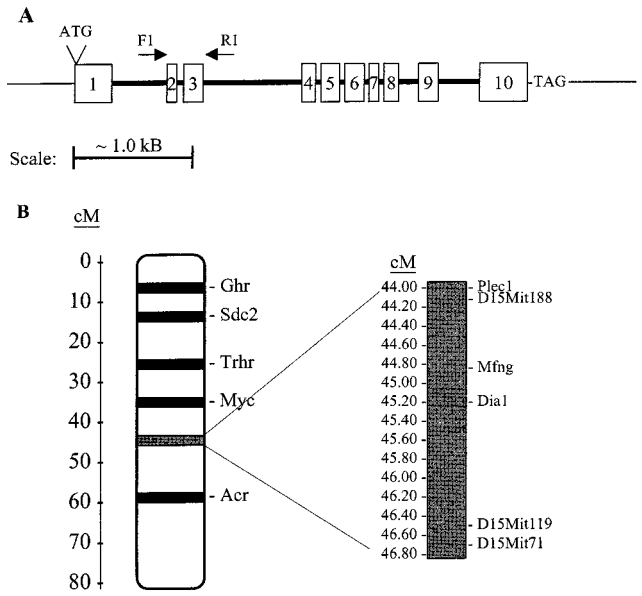

Figure 3 Gene structure and chromosomal location of MYPT3

(**A**) Schematic representation of the gene structure of MYPT3. Highlighted are the exon (boxed) and intron (thick bar) regions spanning 3776 bp. The approximate scaling is shown in kb. The directional arrows indicate the location of a forward (F1) and reverse (R1) primer pair used for radiation hybrid mapping. (**B**) Mouse genetic map indicating the placement of MYPT3 to chromosome 15, approx. 11.32 cR (270 kb per cR_3000) from the marker D15Mit188 [logarithm of the odds ('lod') > 3.0]. Map distances are indicated in cM. Genetic markers shown are cited in the Mouse Genome Database [32].

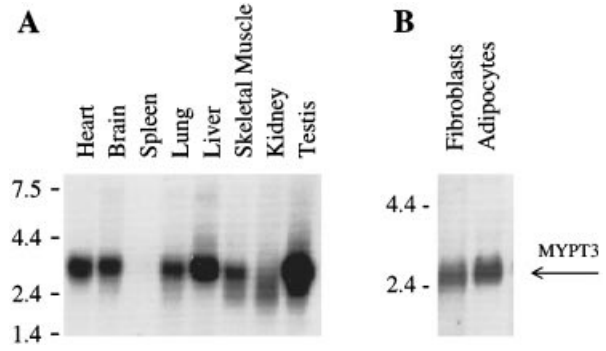

Figure 4 Tissue distribution of MYPT3 mRNA

Northern-blot analysis of MYPT3 mRNA expression in (**A**) multiple mouse tissues and (**B**) 3T3-L1 fibroblasts and differentiated adipocytes. The blots were each hybridized with a 0.5 kb cDNA fragment of MYPT3 generated by restriction digest with *Eco*RI-*Eco*RI as described in the Experimental section. Equal loading of RNA was verified by ethidium bromide staining. The mobility of mRNA size markers (in kb) is indicated on the left of each blot.

testis (Figure 4A). The MYPT3 transcript also was weakly recognized in kidney but was absent from spleen. Similar results were observed for mouse multiple tissue Northern blots hybridized with the complete 1.5 kb MYPT3 cDNA probe (results not shown). Since MYPT3 was isolated from a 3T3-L1 cDNA library, we also performed Northern-blot analysis with both fibroblast and differentiated adipocytes. A single approx. 2.8 kb transcript was found in both 3T3-L1 fibroblasts and differentiated adipocytes, with slight up-regulation during differentiation (Figure 4B). MYPT3 was also detected in Zucker rat white

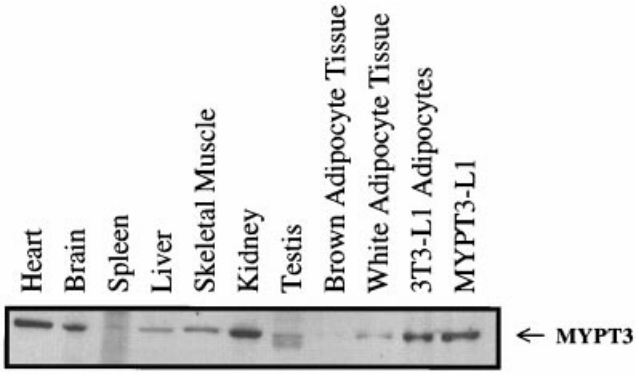

Figure 5 Expression of endogenous MYPT3 in mouse tissue

Cellular extracts of multiple mouse tissues were freshly prepared and fractionated by SDS/PAGE, then transferred to nitrocellulose for immunoblotting as described in the Experimental section. The cellular extract loaded for each tissue was 17.5 μg, except for brown and white adipocyte extracts when 9 μg was loaded. Membranes were probed with an anti-MYPT3 peptide antibody for 1 h at 25 °C. The experiment shown was performed twice with similar results.

adipocytes, skeletal muscle and liver by Northern-blot analysis (results not shown). Overall, these results demonstrate the widespread expression of MYPT3 mRNA in a variety of mouse tissues.

Expression of endogenous MYPT3 in multiple tissues

To determine the expression level of endogenous MYPT3 protein, we prepared cellular extracts from various mouse tissues for Western blotting with an affinity-purified anti-MYPT3 peptide antibody. For antibody production, we synthesized an internal peptide of MYPT3 (shown in Figure 1) based on its antigenicity and insignificant alignment with predicted signalling motifs, various MYPT isoforms, as well as the non-redundant GenBank® peptide database. As shown in Figure 5, MYPT3 was detected predominately in mouse heart, brain and kidney. In addition, MYPT3 was observed in mouse liver, skeletal muscle, testis and white adipocytes; however, little or no MYPT3 was detectable in mouse spleen and brown adipocytes. We also demonstrated that endogenous MYPT3 was detectable in 3T3-L1 differentiated adipocytes (Figure 5). In summary, as predicted from our Northern-blot analysis showing the widespread expression of MYPT3 mRNA, we found that endogenous MYPT3 was expressed in a variety of mouse tissues.

Prenylation of MYPT3

Protein prenylation involves the covalent modification of CaaX-containing and CC- or CxC-containing proteins with either a 15-C farnesyl or 20-C geranylgeranyl isoprenoid. CaaX-containing proteins with a C-terminal serine, methionine or glutamine residue are specifically recognized by farnesyltransferases, whereas a leucine residue specifies modification by geranylgeranyltransferase type I [45,46]. Since MYPT3 contains the residues -CCVLM at the C-terminus, this strongly suggests its potential for farnesylation.

To demonstrate that MYPT3 is prenylatable, we performed *in vitro* assays with purified recombinant HA-Ras, GST–MYPT3 or GST–M110-ΔC in the presence or absence of purified recombinant farnesyltransferase. We expressed full-length MYPT3 as a fusion protein with an N-terminal GST, for affinity purification. The fusion protein was soluble by fermentation at 18 °C, however

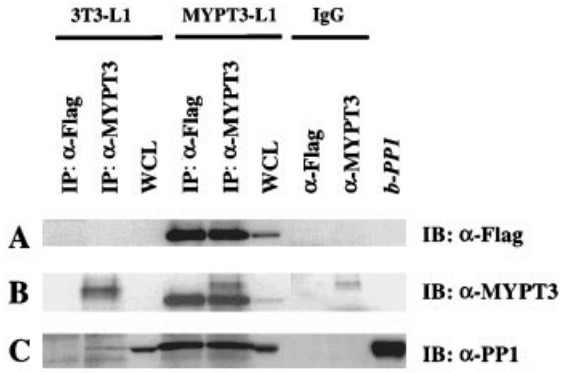

Figure 6 Co-immunoprecipitation of PP1 with MYPT3

Approx. 1.5 mg of 3T3-L1 differentiated adipocyte lysate from either native (3T3-L1) or electroporated (MYPT3-L1) cells containing recombinant FLAG-tagged MYPT3 were subjected to immunoprecipitation by an anti-FLAG monoclonal antibody (α-Flag) or an anti-MYPT3 peptide polyclonal antibody (α-MYPT3). Shown are immunoblots using the (**A**) anti-FLAG M2 monoclonal antibody (IB: α-Flag); (**B**) anti-MYPT3 peptide antibody (IB: α-MTPT3); (**C**) anti-PP1 polyclonal antibody (IB: α-PP1). WCL, whole cell lysate. IgG (controls) and *b-PP1* (bacterial lysate containing recombinant PP1) are shown on the right. The results are representative of at least three experiments.

was insoluble under various growth and induction conditions at 25 °C, 30 °C, and 37 °C (results not shown). After affinity chromatography on glutathione–agarose, the final product contained a 85000 Da (fusion protein) and a 27000 Da (free GST) polypeptide, in an approx. 50:50 ratio, when analysed by SDS/PAGE and staining with Coomassie Blue. Following a 30 min prenylation reaction at 37 °C, we measured the incorporation of [^{3}H]FPP into protein samples using a standard filter-binding assay and liquid scintillation counting of the dried filters. We observed that the purified recombinant GST–MYPT3 incorporated [^{3}H]FPP in the presence of farnesyltransferase, but not in its absence. The specific activity for farnesylation of GST–MYPT3 was approx. 2.3 pmol of FPP incorporated/h. Incorporation of [^{3}H]FPP into HA-tagged Ras was observed only in the presence of farnesyltransferase, having an approx. specific activity of 5.0 pmol of FPP incorporated/h. Since purified recombinant HA-Ras contains the C-terminus CVLS, which is a reported farnesyltransferase substrate [35], this sample serves as a positive control. A recombinant 72.5 kDa fragment of the rat kidney M110 subunit, an isoform of MYPT1, was expressed in bacteria as an N-terminal GST fusion protein lacking any predicted prenylation motifs. Assays using GST–M110-ΔC as substrate showed only background levels of bound isotope in the presence or absence of farnesyltransferase, consistent with the use of this negative control (results not shown). Overall, since MYPT3 serves as a substrate for purified farnesyltransferase *in vitro*, these results support the prediction that MYPT3 is a prenylatable protein.

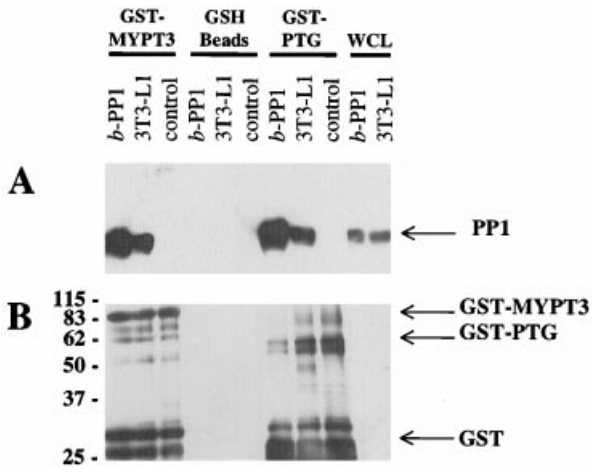

Figure 7 GST–MYPT3 binds the catalytic subunit of PP1

Immobilized GST–MYPT3, GST–PTG or glutathione-Sepharose beads alone were incubated for 60 min at 4 °C with bacterial lysate overexpressing recombinant PP1 (*b*-PP1), 3T3-L1 differentiated adipocytes (3T3-L1) or buffer alone (control). (**A**) Samples were subjected to SDS/PAGE and immunoblotting with polyclonal PP1 antibody. (**B**) The blot was stripped and then re-probed with anti-GST antibodies. Molecular mass markers (kDa) are indicated on the left. Arrows indicate bands corresponding to GST–MYPT3, GST–PTG, GST, and PP1. Results are representative of three independent experiments.

Interaction of MYPT3 with mammalian PP1

To determine whether MYPT3 interacts with endogenous PP1 from mammalian cells, we subjected Triton-soluble lysates from 3T3-L1 differentiated adipocytes to immunoprecipitation, using an anti-FLAG M2 monoclonal antibody or an anti-peptide MYPT3 antibody. In addition, lysates from 3T3-L1 adipocytes, electroporated with an N-terminal FLAG-tagged MYPT3 and harvested 48 h later, were also subjected to similar immunoprecipitation. Following extensive washing, immunoprecipitates were subjected to SDS/PAGE and immunoblotting with an anti-FLAG M2 monoclonal antibody, then stripped and re-probed with an anti-MYPT3 peptide-antibody or with an anti-PP1 antibody. Immunoblots with the anti-FLAG M2 antibody revealed a single polypeptide of 75 kDa, immunoprecipitated by both the anti-FLAG M2 and anti-MYPT3 peptide antibody from 3T3-L1 lysate containing recombinant MYPT3 (Figure 6A). A single corresponding 75 kDa band was also detected in 3T3-L1 lysates containing recombinant MYPT3. Since a corresponding band in non-transfected 3T3-L1 cells or IgG control samples was not found, these immunoblots demonstrate the specificity of the M2 antibody for FLAG-tagged MYPT3. These results also suggest that the anti-MYPT3 peptide antibody is capable of immunoprecipitating FLAG-tagged MYPT3. To confirm the identity of MYPT3, we stripped blots and re-probed with the anti-MYPT3 peptide antibody. We observed a corresponding single polypeptide of approx. 75 kDa, immunoprecipitated by either anti-FLAG or anti-MYPT3 peptide antibody from 3T3-L1 cells containing recombinant FLAG-MYPT3 (Figure 6B). When native lysate was subjected to immunoprecipitation using the anti-FLAG antibody and was immunoblotted with anti-MYPT3 antibody, no bands were seen. However, a 75 kDa polypeptide was immunoprecipitated from native lysates by the anti-MYPT3 peptide antibody (Figure 6B). When immunoblotted with anti-MYPT3, we also routinely observed a single 75 kDa polypeptide in whole lysates from 3T3-L1 cells; however it was found only in lysates containing the recombinant protein under the conditions used in these studies (Figure 6B). Interestingly, MYPT3 migrated more slowly than would be expected from its predicted molecular mass of 58 kDa, quite possibly due to covalent modification by prenylation. These results clearly demonstrate the capability and specificity of the anti-MYPT3 peptide antibody to immunoprecipitate MYPT3. In all cases where MYPT3 was immunoprecipitated from native or electroporated 3T3-L1 cells, immunoblotting with anti-PP1 antibody revealed a single 37 kDa band (Figure 6C). The band

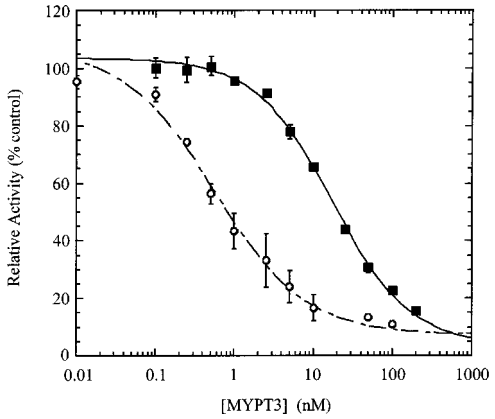

Figure 8 Inhibition, *in vitro*, of PP1 activity by MYPT3

Purified recombinant human PP1γ catalytic subunit was assayed for 15 min at 30 °C with either 5 μM ^{32}P-labelled phosphorylase *a* (○) or 20 μM ^{32}P-labelled MLC (■) and increasing concentrations of affinity-purified GST–MYPT3, as described in the Experimental section. Data are shown as the activity relative to control in the absence of MYPT3. Specific activity for samples without MYPT3 was approx. 2750 nmol and 80 nmol of P_i released per min/mg of protein for phosphorylase and MLC respectively. The values shown are the means ± S.E.M. from three independent experiments, which were performed in triplicate for each substrate.

was much weaker in immune complexes from native lysates when compared with 3T3-L1 cells overexpressing MYPT3. A corresponding 37 kDa polypeptide was detectable in 3T3-L1 whole-cell lysates, and in bacterial lysates containing recombinant PP1, but was absent from immune complexes from native 3T3-L1 cells subjected to immunoprecipitation with anti-FLAG antibody (Figure 6C). Similar experiments using CHO/IR (Chinese Hamster ovary cells stably transfected with insulin receptor) lysates also indicated that immunoprecipitated MYPT3 interacts with PP1 *in vivo* (results not shown). Overall, these experiments demonstrated that both endogenous and FLAG-tagged MYPT3 co-immunoprecipitate with PP1.

To confirm the interaction of MYPT3 and PP1, we also performed *in vitro* pull-down experiments with immobilized GST–MYPT3, using 3T3-L1 differentiated adipocyte lysates. These experiments were conducted in parallel with glutathione–Sepharose beads alone or with immobilized GST–PTG, using a pre-cleared bacterial lysate containing overexpressed PP1, the 3T3-L1 lysate or a buffer control. After incubation with lysate for 60 min, samples were washed extensively and subjected to SDS/PAGE and immunoblotting with either an anti-PP1 antibody or anti-GST-antibody. Immunoblots with an anti-PP1 antibody revealed the presence of a single 37 kDa polypeptide in both the bacterial and 3T3-L1 adipocyte lysates which had been subjected to GST–MYPT3 pull-downs, but not in the buffer control sample, suggesting the specific interaction of GST–MYPT3 with PP1 (Figure 7A). The anti-PP1 antibody failed to detect the presence of any bands from samples subjected to pull-down with the glutathione–Sepharose beads alone, confirming that the interaction of GST–MYPT3 was not due to the beads (Figure 7A). As a positive control, both the bacterial and 3T3-L1 lysates subjected to pull-downs with GST–PTG contained a single polypeptide with an apparent molecular mass of 37 kDa after immunoblotting with the anti-PP1 antibody. A single 37 kDa polypeptide was also detected in whole lysates, thus confirming the identification of PP1 (Figure 7A). When blots were stripped and re-probed with an anti-GST antibody, we observed approximately equal loading of each GST fusion protein and GST in samples, except for those containing beads alone or whole lysates (Figure 7B). The specific interaction of GST–MYPT3 with PP1 from CHO/IR lysates was also observed in similar reproducible experiments (results not shown). Likewise, in similar experiments using lysates from ^{35}S-labelled 3T3-L1 differentiated adipocytes, autoradiography revealed the presence of only a 37 kDa protein in pull-downs with GST–MYPT3, but not with the buffer control, GST or glutathione–Sepharose beads alone. Immunoblotting with an anti-PP1 antibody confirmed the identification of the 37 kDa protein as the catalytic subunit (results not shown). Overall, we observed a specific interaction of PP1 with GST–MYPT3 *in vitro*, thus supporting the model of MYPT3 as a phosphatase subunit.

Inhibition of PP1 activity by MYPT3

Previously identified MYPT family members inhibit PP1 activity with phosphorylase *a* as substrate, but activate PP1 toward myosin *in vitro* [18,47,48]. To determine the effect of MYPT3 on PP1 activity, we performed phosphatase assays with a highly purified recombinant PP1 catalytic subunit (γ-isoform) and affinity-purified recombinant MYPT3 (full-length, residues 1–524) fused to GST at the N-terminal. When assayed with 5 μM ^{32}P-labelled phosphorylase *a*, purified recombinant GST–MYPT3 inhibited PP1 activity in a concentration-dependent manner (Figure 8). Half-maximal inhibition occurred at approx. 0.6 nM GST–MYPT3. Purified GST–MYPT3 also inhibited the activity of PP1 toward 20 μM ^{32}P-labelled MLC. Concentration-dependent inhibition of PP1 activity toward MLC was approx. 17.4 nM GST–MYPT3 (Figure 8). The increased IC_{50} observed in MLC assays may be partly due to higher concentrations of PP1 (7.5 nM) compared with that used in phosphorylase assays (1 nM). In control experiments, phosphatase activity toward MLC was blocked approx. 80 % by 200 nM GST–MYPT3, whereas GST–M110-ΔC failed to inhibit activity in a manner consistent with previous reports (results not shown). We also observed that 200 nM GST–MYPT3 completely inhibited phosphatase activity toward 1 μM ^{32}P-labelled myosin, whereas GST–M110-ΔC did not inhibit activity (results not shown). Together, these studies suggest that MYPT3 specifically inhibits PP1 activity toward phosphorylase, MLC and myosin, thus differentiating this protein from other MYPT family members.

DISCUSSION

PP1 is a ubiquitously expressed serine/threonine phosphatase that resides in most cellular compartments and has broad substrate specificity *in vitro*, suggesting the necessity for its precise regulation. The catalytic subunit of PP1 is mainly regulated by distinct regulatory protein subunits that directly inhibit activity or target the enzyme to specific subcellular compartments or substrates [2,4]. Interestingly, several of the known subunits have homologous structures, yet also contain distinct regions that may allow differential regulation or targetting of PP1. Although more than 20 subunits have been discovered, the mechanisms of PP1 compartmentalization remain incompletely described, since the reported subunits do not fully account for the diverse intracellular actions of PP1. Thus it remains important to identify novel subunits to gain a better understanding of the compartmentalized regulation of PP1.

To identify novel PP1-interacting proteins, we screened a 3T3-L1 adipocyte cDNA library with PP1 as bait, using the yeast

two-hybrid method. In this report, we describe the cloning and initial biochemical characterization of the previously unidentified PP1-interacting protein, MYPT3, and its identification as a member of the MYPT family. Previous studies have classified two distinct genes in the MYPT family, identified as *MYPT1* and *MYPT2* (for a review see [49]). Both genes encode several ~ 110–130 kDa isoforms derived from alternative splicing. An additional gene, *Mel-11*, was identified in *C. elegans*, and encodes for a 110 kDa product that is approx. 35% identical with MYPT1/2 [50]. MYPT3 aligns > 99% with a region of genomic DNA from mouse clone RP23-156P23 and localizes to chromosome 15, between markers at 44.0–45.5 cM, as demonstrated in the present work by radiation hybrid mapping. In contrast, *in situ* hybridization analysis localizes the 4.8 kb *MYPT1* and the 3.8 kb *MYPT2* gene to human chromosome 12q15-q21 and 1q32.1 respectively [41,42]. In the present study, we identify the 3.8 kb coding region, comprising 10 exons encoding for a 524-amino-acid sequence with a predicted molecular mass of 57529 Da. Based on the alignment of MYPT3 with several working draft sequences of human genomic clones, our observations also raise the possibility of additional genes related to *MYPT*3. We also observed homology of MYPT3 with deduced proteins from previously unidentified genomic sequence including the human KIAA0823, *Drosophila* CG6896, and *C. elegans* K02A11 gene products. Each gene product contains a potential -CC or -CaaX prenylation motif, a potential ATP/GTP binding motif, and multiple ankyrin repeats. Overall, we have cloned a distinct mouse myosin phosphatase targetting subunit, MYPT3, and observed its homology with several deduced gene products from other species, suggesting the identification of a novel subfamily of prenylatable MYPT subunits.

Amino acid alignments reveal that MYPT3 is approx. 30–40% identical, and therefore homologous, with the MYPT family. One homologous feature of MYPTs and other PP1 targetting subunits, is the conservation of the residues [K/R]-[V/I]-X-F that define the consensus PP1-binding site [43]. Importantly, MYPT3 exhibits a similar consensus site (V-X-F) near its N-terminus and binds PP1 *in vivo*, as determined by the yeast two-hybrid analysis, as well as co-immunoprecipitation with either endogenous or overexpressed MYPT3. They also interact *in vitro* in pull-down experiments with GST–MYPT3. Another homologous feature of MYPT1/2, is the multiple ankyrin repeats that dominate the N-terminal region (residues 1–296). Ankyrin repeats are tandemly repeated motifs of approx. 33 residues that occur in numerous proteins of diverse function and may function in protein–protein interactions (for a review see [51]). Several crystal and solution structures have shown that an ankyrin repeat contains a conserved L-shaped structure with a β-hairpin and two α-helices [52–55]. The N-terminal residues 1–374 of MYPT1/2 are critical for the activation of myosin phosphatase activity [18,48], and are approx. 30–40% identical with MYPT3. Interestingly, MYPT3 specifically inhibits PP1 activity toward phosphorylase, MLC and myosin *in vitro*. When assayed with phosphorylase, the concentration-dependent inhibition by MYPT3 (IC_{50} ~ 0.6 nM) is approximately equal to values reported for MYPT2 [48], consistent with this as a general biochemical property of the MYPT family. However, in contrast with phosphorylase *a* as substrate, both MYPT1/2 stimulated the dephosphorylation of myosin and MLC [18,48], a feature opposite to that observed with MYPT3. These findings suggest a different function for MYPT3, but the significance of this finding is uncertain. In a model proposed previously, it is suggested that an unidentified C-terminal region may also be involved in the activation of myosin/MLC activity by MYPT1/2 [56]. The binding of the 20 kDa subunit via the C-terminal region of MYPT1/2 was not required for PP1 activation [18,48]. Although MYPT1/2 normally exist in a heterotrimeric complex with PP1 and M20 *in vivo*, we have not observed additional MYPT3 binding proteins, other than PP1. Based on its sequence, MYPT3 does not appear to contain the C-terminal region found in MYPT, which is proposed to bind the 20 kDa subunit. Interestingly, the unique inhibitory action of MYPT3 suggests that its distinct C-terminal region may contribute to substrate or subunit binding in a manner significantly different from MYPT1/2. Since MYPT3 lacks the C-terminal region found in MYPT1/2, this structural difference may partially account for the inhibition of PP1 activity observed *in vitro*. In addition, since ankyrin repeats may mediate diverse protein–protein interactions, it remains a possibility that an unidentified protein may be preferred by MYPT3 as the physiological substrate. Further mechanistic studies will be necessary to understand the difference between MYPT3 and MYPT1/2 regarding myosin binding and dephosphorylation by PP1.

The regulation of myosin phosphorylation is an important mechanism controlling muscular contraction, induction of stress fibre formation and focal adhesion formation in fibroblasts, and neurite retraction in neuronal cells [57–60] (but see also [60a]). Calcium-activated MLC kinase or Rho-associated kinase ('ROCK'), which are activated by the small GTPase Rho, phosphorylate MYPT1/2, which leads to the inhibition of PP1 activity toward MLC [17,61–63]. The major protein phosphatase that dephosphorylates myosin has been described as a heterotrimer containing the PP1 catalytic subunit, an approx. 110–130 kDa MYPT, and a 20 kDa protein of unknown function (for a review see [49]). However, as described here, the 58 kDa MYPT homologue may also play a role in the regulation of myosin phosphorylation. Since a 58 kDa 'proteolytic product' has been observed in various reports on MYPT1 and MYPT2 [19,20,64], it is important to determine whether MYPT3 is present and can simultaneously bind PP1 in these systems. It will also be of interest to know whether MYPT3 binds to Rho GTPases and is regulated by phosphorylation.

The tissue or subcellular localization of respective MYPT subunits may contribute to the regulation of myosin phosphorylation. MYPT3 mRNA is widely expressed in various mouse tissues, as well as in 3T3-L1 fibroblasts and differentiated adipocytes. While MYPT3 and MYPT2 are ubiquitously expressed, MYPT1 mRNA is found mainly in heart and brain [41,42]. However, even if found in the same tissue type, it remains to be seen if MYPT3 locates to the same subcellular compartments as MYPT1/2. In preliminary fractionation studies, we found MYPT3 in both the microsomal membrane fraction and cytosol, but not in the plasma membrane or caveolae.

MYPT3 differs significantly from related MYPT subunits at its C-terminal region. MYPT3 is approximately one-half the molecular mass of the known 107–115 kDa MYPT subunits, and lacks the putative regulatory phosphorylation sites at Thr-654/Thr-695 and the leucine-zipper motif found in MYPT2. In contrast, the C-terminal region of MYPT3 contains several distinct signalling motifs that are absent from MYPT1/2, including a putative ATP/GTP-binding motif [65,66] and two independent SH3-binding consensus sites (class I), suggesting the potential for regulation by nucleotides or other interacting proteins. Most interesting are the potential prenylation -CC and -CaaX motifs at the C-terminus of MYPT3. We have shown that MYPT3 is prenylated by purified recombinant farnesyltransferase *in vitro*. The -CC motif of MYPT3 indicates the potential for additional lipid modification following prenylation of the C-terminal cysteine residue *in vivo*. Prenylation of MYPT3

may significantly contribute to its regulation by subcellular localization, and allow for regulation by protein–protein interactions, as is known for other prenylatable proteins [45,46]. Thus MYPT3 has a distinct regulatory activity *in vitro*, and has structural motifs which are uncharacteristic of known MYPT family members, suggesting its potentially unique role in the regulation of myosin phosphorylation and the subsequent regulation of downstream events in the cell.

The authors thank Shian-Huey Chiang, Dr Matthew Brady, Dr Shirish Shenolikar and Dr Greg Taylor for valuable discussions and assistance. We thank Dr Pat Casey, Dr Tim Haystead and Dr John Lawrence Jr. for generously providing reagents. Our appreciation goes to Dr Archana Chaudhry and Chen Zhang for mouse tissues. We also thank Frank Bourbonais and Kris Blanchard for their technical assistance in protein expression and Northern blot analysis respectively.

REFERENCES

1 Shenolikar, S. (1994) Protein serine/threonine phosphatases – new avenues for cell regulation. Annu. Rev. Cell Biol. **10**, 55–86
2 Aggen, J. B., Nairn, A. C. and Chamberlin, R. (2000) Regulation of protein phosphatase-1. Chem. Biol. **7**, R13–R23
3 Hubbard, M. J. and Cohen, P. (1993) On target with a new mechanism for the regulation of protein phosphorylation. Trends Biochem. Sci. **18**, 172–177
4 Faux, M. C. and Scott, J. D. (1996) More on target with protein phosphorylation: conferring specificity by location. Trends Biochem. Sci. **21**, 312–315
5 Cohen, P. (1989) The structure and regulation of protein phosphatases. Annu. Rev. Biochem. **58**, 453–508
6 Cohen, P., Foulkes, J. G., Holmes, C. F., Nimmo, G. A. and Tonks, N. K. (1988) Protein phosphatase inhibitor-1 and inhibitor-2 from rabbit skeletal muscle. Methods Enzymol. **159**, 427–437
7 Matovcik, L. M., Hemmings, Jr., H. C. and Kinder, B. K. (1995) DARPP-32 (dopamine and cAMP-regulated phosphoprotein, M(r) 32,000) is a membrane protein in the bovine parathyroid. FEBS Lett. **364**, 67–74
8 Beullens, M., Van Eynde, A., Stalmans, W. and Bollen, M. (1992) The isolation of novel inhibitory polypeptides of protein phosphatase 1 from bovine thymus nuclei. J. Biol. Chem. **267**, 16538–16544
9 Van Eynde, A., Wera, S., Beullens, M., Torrekens, S., Van Leuven, F., Stalmans, W. and Bollen, M. (1995) Molecular cloning of NIPP-1, a nuclear inhibitor of protein phosphatase-1, reveals homology with polypeptides involved in RNA processing. J. Biol. Chem. **270**, 28068–28074
10 Doherty, M. J., Moorhead, G., Morrice, N., Cohen, P. and Cohen, P. T. (1995) Amino acid sequence and expression of the hepatic glycogen-binding (GL) subunit of protein phosphatase-1. FEBS Lett. **375**, 294–298
11 Moorhead, G., MacKintosh, C., Morrice, N. and Cohen, P. (1995) Purification of the hepatic glycogen-associated form of protein phosphatase-1 by microcystin-Sepharose affinity chromatography. FEBS Lett. **362**, 101–105
12 Hubbard, M. J. and Cohen, P. (1989) The glycogen-binding subunit of protein phosphatase-1G from rabbit skeletal muscle. Further characterisation of its structure and glycogen-binding properties. Eur. J. Biochem. **180**, 457–465
13 Tang, P. M., Bondor, J. A., Swiderek, K. M. and DePaoli-Roach, A. A. (1991) Molecular cloning and expression of the regulatory (RG1) subunit of the glycogen-associated protein phosphatase. J. Biol. Chem. **266**, 15782–15789
14 Printen, J. A., Brady, M. J. and Saltiel, A. R. (1997) PTG, a protein phosphatase 1-binding protein with a role in glycogen metabolism. Science **275**, 1475–1478
15 Allen, P. B., Kwon, Y. G., Nairn, A. C. and Greengard, P. (1998) Isolation and characterization of PNUTS, a putative protein phosphatase 1 nuclear targeting subunit. J. Biol. Chem. **273**, 4089–4095
16 Chen, Y. H., Chen, M. X., Alessi, D. R., Campbell, D. G., Shanahan, C., Cohen, P. and Cohen, P. T. (1994) Molecular cloning of cDNA encoding the 110 kDa and 21 kDa regulatory subunits of smooth muscle protein phosphatase 1 M. FEBS Lett. **356**, 51–55
17 Kimura, K., Ito, M., Amano, M., Chihara, K., Fukata, Y., Nakafuku, M., Yamamori, B., Feng, J., Nakano, T., Okawa, K., Iwamatsu, A. and Kaibuchi, K. (1996) Regulation of myosin phosphatase by Rho and Rho-associated kinase (Rho-kinase). Science **273**, 245–248
18 Haystead, C. M., Gailly, P., Somlyo, A. P., Somlyo, A. V. and Haystead, T. A. (1995) Molecular cloning and functional expression of a recombinant 72.5 kDa fragment of the 110 kDa regulatory subunit of smooth muscle protein phosphatase 1 M. FEBS Lett. **377**, 123–127
19 Okubo, S., Ito, M., Takashiba, Y., Ichikawa, K., Miyahara, M., Shimizu, H., Konishi, T., Shima, H., Nagao, M., Hartshorne, D. J. et al. (1994) A regulatory subunit of smooth muscle myosin bound phosphatase. Biochem. Biophys. Res. Commun. **200**, 429–434
20 Shimizu, H., Ito, M., Miyahara, M., Ichikawa, K., Okubo, S., Konishi, T., Naka, M., Tanaka, T., Hirano, K., Hartshorne, D. J. et al. (1994) Characterization of the myosin-binding subunit of smooth muscle myosin phosphatase. J. Biol. Chem. **269**, 30407–30411
21 Kennelly, P. J., Edelman, A. M., Blumenthal, D. K. and Krebs, E. G. (1987) Rabbit skeletal muscle myosin light chain kinase. The calmodulin binding domain as a potential active site-directed inhibitory domain. J. Biol. Chem. **262**, 11958–11963
22 Ulbricht, B. and Soldati, T. (1999) Production of reagents and optimization of methods for studying calmodulin-binding proteins. Protein Expression Purif. **15**, 24–33
23 Brady, M. J., Printen, J. A., Mastick, C. C. and Saltiel, A. R. (1997) Role of protein targeting to glycogen (PTG) in the regulation of protein phosphatase-1 activity. J. Biol. Chem. **272**, 20198–20204
24 Ribon, V., Printen, J. A., Hoffman, N. G., Kay, B. K. and Saltiel, A. R. (1998) A novel, multifuntional c-Cbl binding protein in insulin receptor signalling in 3T3-L1 adipocytes. Mol. Cell. Biol. **18**, 872–879
25 Altschul, S. F., Gish, W., Miller, W., Myers, E. W. and Lipman, D. J. (1990) Basic local alignment search tool. J. Mol. Biol. **215**, 403–410
26 Altschul, S. F., Madden, T. L., Schaffer, A. A., Zhang, J., Zhang, Z., Miller, W. and Lipman, D. J. (1997) Gapped BLAST and PSI-BLAST: a new generation of protein database search programs. Nucleic Acids Res. **25**, 3389–3402
27 Schultz, J., Copley, R. R., Doerks, T., Ponting, C. P. and Bork, P. (2000) SMART: a web-based tool for the study of genetically mobile domains. Nucleic Acids Res. **28**, 231–234
28 Ponting, C. P., Schultz, J., Milpetz, F. and Bork, P. (1999) SMART: identification and annotation of domains from signalling and extracellular protein sequences. Nucleic Acids Res. **27**, 229–232
29 Hofmann, K., Bucher, P., Falquet, L. and Bairoch, A. (1999) The PROSITE database, its status in 1999. Nucleic Acids Res. **27**, 215–219
30 Bateman, A., Birney, E., Durbin, R., Eddy, S. R., Howe, K. L. and Sonnhammer, E. L. (2000) The Pfam protein families database. Nucleic Acids Res. **28**, 263–266
31 McCarthy, L. C., Terrett, J., Davis, M. E., Knights, C. J., Smith, A. L., Critcher, R., Schmitt, K., Hudson, J., Spurr, N. K. and Goodfellow, P. N. (1997) A first-generation whole genome-radiation hybrid map spanning the mouse genome. Genome Res. **7**, 1153–1161
32 Blake, J. A., Eppig, J. T., Richardson, J. E. and Davisson, M. T. (2000) The Mouse Genome Database (MGD): expanding genetic and genomic resources for the laboratory mouse. The Mouse Genome Database Group. Nucleic Acids Res. **28**, 108–111
33 Chomcynski, P. and Sacchi, N. (1987) Single-step method of RNA isolation by acid guanidinium thiocyanate-phenol-chloroform extraction. Anal. Biochem. **162**, 156–159
34 Bradford, M. M. (1976) A rapid and sensitive method for the quantitation of microgram quantities of protein utilizing the principle of protein-dye binding. Anal. Biochem. **72**, 248–254
35 Reiss, Y., Goldstein, J. L., Seabra, M. C., Casey, P. J. and Brown, M. S. (1990) Inhibition of purified p21ras farnesyl:protein transferase by Cys-AAX tetrapeptides. Cell **62**, 81–88
36 Thissen, J. A. and Casey, P. J. (1996) Kinetics of protein farnesyltransferase: sigmoidal vs hyperbolic behavior as a function of assay conditions. Anal. Biochem. **243**, 80–85
37 Lazar, D. F., Wiese, R. J., Brady, M. J., Mastick, C. C., Waters, S. B., Yamauchi, K., Pessin, J. E., Cuatrecasas, P. and Saltiel, A. R. (1995) Mitogen-activated protein kinase kinase inhibition does not block the stimulation of glucose utilization by insulin. J. Biol. Chem. **270**, 20801–20807
38 Min, J., Okada, S., Kanzaki, M., Elmendorf, J. S., Coker, K. J., Ceresa, B. P., Syu, L. J., Noda, Y., Saltiel, A. R. and Pessin, J. E. (1999) Synip: a novel insulin-regulated syntaxin 4-binding protein mediating GLUT4 translocation in adipocytes [published erratum appears in Mol. Cell (1999) **4(1)**:following 192]. Mol. Cell **3**, 751–760
39 Kozak, M. (1996) Interpreting cDNA sequences: some insights from studies on translation. Mamm. Genome **7**, 563–574
40 Kozak, M. (1984) Compilation and analysis of sequences upstream from the translational start site in eukaryotic mRNAs. Nucleic Acids Res. **12**, 857–872
41 Takahashi, N., Ito, M., Tanaka, J., Nakano, T., Kaibuchi, K., Odai, H. and Takemura, K. (1997) Localization of the gene coding for myosin phosphatase, target subunit 1 (MYPT1) to human chromosome 12q15-q21. Genomics **44**, 150–152
42 Fujioka, M., Takahashi, N., Odai, H., Araki, S., Ichikawa, K., Feng, J., Nakamura, M., Kaibuchi, K., Hartshorne, D. J., Nakano, T. and Ito, M. (1998) A new isoform of human myosin phosphatase targeting/regulatory subunit (MYPT2): cDNA cloning, tissue expression, and chromosomal mapping. Genomics **49**, 59–68
43 Egloff, M. P., Johnson, D. F., Moorhead, G., Cohen, P. T., Cohen, P. and Barford, D. (1997) Structural basis for the recognition of regulatory subunits by the catalytic subunit of protein phosphatase 1. EMBO J. **16**, 1876–1887
44 Ichikawa, K., Ito, M. and Hartshorne, D. J. (1996) Phosphorylation of the large subunit of myosin phosphatase and inhibition of phosphatase activity. J. Biol. Chem. **271**, 4733–4740

45 Fu, H. W. and Casey, P. J. (1999) Enzymology and biology of CaaX protein prenylation. Recent Prog. Horm. Res. **54**, 315–342
46 Zhang, F. L. and Casey, P. J. (1996) Protein prenylation: molecular mechanisms and functional consequences. Ann. Rev. Biochem. **65**, 241–269
47 Ichikawa, K., Hirano, K., Ito, M., Tanaka, J., Nakano, T. and Hartshorne, D. J. (1996) Interactions and properties of smooth muscle myosin phosphatase. Biochemistry **35**, 6313–6320
48 Hirano, K., Phan, B. C. and Hartshorne, D. J. (1997) Interactions of the subunits of smooth muscle myosin phosphatase. J. Biol. Chem. **272**, 3683–3688
49 Hartshorne, D. J., Ito, M. and Erdodi, F. (1998) Myosin light chain phosphatase: subunit composition, interactions and regulation. J. Muscle Res. Cell Motil. **19**, 325–341
50 Wissmann, A., Ingles, J., McGhee, J. D. and Mains, P. E. (1997) *Caenorhabditis elegans* LET-502 is related to Rho-binding kinases and human myotonic dystrophy kinase and interacts genetically with a homolog of the regulatory subunit of smooth muscle myosin phosphatase to affect cell shape. Genes Dev. **11**, 409–422
51 Sedgwick, S. G. and Smerdon, S. J. (1999) The ankyrin repeat: a diversity of interactions on a common structural framework. Trends Biochem. Sci. **24**, 311–316
52 Gorina, S. and Pavletich, N. P. (1996) Structure of the p53 tumor suppressor bound to the ankyrin and SH3 domains of 53BP2. Science **274**, 1001–1005
53 Batchelor, A. H., Piper, D. E., de la Brousse, F. C., McKnight, S. L. and Wolberger, C. (1998) The structure of GABPalpha/beta: an ETS domain- ankyrin repeat heterodimer bound to DNA. Science **279**, 1037–1041
54 Jacobs, M. D. and Harrison, S. C. (1998) Structure of an IkappaBalpha/NF-kappaB complex. Cell **95**, 749–758
55 Luh, F. Y., Archer, S. J., Domaille, P. J., Smith, B. O., Owen, D., Brotherton, D. H., Raine, A. R., Xu, X., Brizuela, L., Brenner, S. L. and Laue, E. D. (1997) Structure of the cyclin-dependent kinase inhibitor p19Ink4d. Nature (London) **389**, 999–1003
56 Johnson, D., Cohen, P., Chen, M. X., Chen, Y. H. and Cohen, P. T. (1997) Identification of the regions on the M110 subunit of protein phosphatase 1 M that interact with the M21 subunit and with myosin. Eur. J. Biochem. **244**, 931–939

Received 18 January 2001/5 February 2001; accepted 8 March 2001

57 Kaibuchi, K., Kuroda, S. and Amano, M. (1999) Regulation of the cytoskeleton and cell adhesion by the Rho family GTPases in mammalian cells. Annu. Rev. Biochem. **68**, 459–486
58 Hartshorne, D. J. (1987) In Physiology of the Gastrointestinal Tract (Johnson, L. R., ed.), pp. 423–482, Raven Press, New York
59 Burridge, K. and Chrzanowska-Wodnicka, M. (1996) Focal adhesions, contractility, and signalling. Annu. Rev. Cell. Dev. Biol. **12**, 463–518
60 Somlyo, A. P. and Somlyo, A. V. (1994) Signal transduction and regulation in smooth muscle. Nature (London) **372**, 231–236
60a Somlyo, A. P. and Somlyo, A. V. (1994) Erratum. Nature (London) **372**, 812
61 Amano, M., Ito, M., Kimura, K., Fukata, Y., Chihara, K., Nakano, T., Matsuura, Y. and Kaibuchi, K. (1996) Phosphorylation and activation of myosin by Rho-associated kinase (Rho-kinase). J. Biol. Chem. **271**, 20246–20249
62 Feng, J., Ito, M., Ichikawa, K., Isaka, N., Nishikawa, M., Hartshorne, D. J. and Nakano, T. (1999) Inhibitory phosphorylation site for Rho-associated kinase on smooth muscle myosin phosphatase. J. Biol. Chem. **274**, 37385–37390
63 Trinkle-Mulcahy, L., Ichikawa, K., Hartshorne, D. J., Siegman, M. J. and Butler, T. M. (1995) Thiophosphorylation of the 130-kDa subunit is associated with a decreased activity of myosin light chain phosphatase in alpha-toxin-permeabilized smooth muscle. J. Biol. Chem. **270**, 18191–18194
64 Hirano, M., Niiro, N., Hirano, K., Nishimura, J., Hartshorne, D. J. and Kanaide, H. (1999) Expression, subcellular localization, and cloning of the 130-kDa regulatory subunit of myosin phosphatase in porcine aortic endothelial cells. Biochem. Biophys. Res. Commun. **254**, 490–496
65 Saraste, M., Sibbald, P. R. and Wittinghofer, A. (1990) The P-loop – a common motif in ATP- and GTP-binding proteins. Trends Biochem. Sci. **15**, 430–434
66 Walker, J. E., Saraste, M., Runswick, M. J. and Gay, N. J. (1982) Distantly related sequences in the alpha- and beta-subunits of ATP synthase, myosin, kinases and other ATP-requiring enzymes and a common nucleotide binding fold. EMBO J. **1**, 945–951